Intel Serv Robotics (2009) 2:219–231
DOI 10.1007/s11370-009-0046-7

SPECIAL ISSUE

# Simultaneous localization of multiple unknown CSMA-based wireless sensor network nodes using a mobile robot with a directional antenna

**Jingang Yi · Chang-Young Kim · Dezhen Song**

Received: 3 April 2009 / Accepted: 28 July 2009 / Published online: 23 August 2009


**Abstract** We use a single mobile robot equipped with a directional antenna to simultaneously localize unknown carrier sensing multiple access (CSMA)-based wireless sensor network nodes. We assume the robot can only sense radio transmissions at the physical layer. The robot does not know network configuration such as size and protocol. We formulate this new localization problem and propose a particle filter-based localization approach. We combine a CSMA model and a directional antenna model using multiple particle filters. The CSMA model provides network configuration data while the directional antenna model provides inputs for particle filters to update. Based on the particle distribution, we propose a robot motion planning algorithm that assists the robot to efficiently traverse the field to search radio source. The final localization scheme consists of two algorithms: a sensing algorithms that runs in $O(n)$ time for $n$ particles and a motion planning algorithm that runs in $O(nl)$ time for $l$ radio sources. We have implemented the algorithm, and the results show that the algorithms are capable of localizing unknown networked radio sources effectively and robustly.

This work was supported in part by the National Science Foundation under grant IIS-0643298.

J. Yi (✉)
Mechanical and Aerospace Engineering Department,
Rutgers University, Piscataway, NJ 08854, USA
e-mail: jgyi@rutgers.edu

C.-Y. Kim · D. Song
Computer Science and Engineering Department,
Texas A&M University, College Station,
TX 77843, USA
e-mail: kcyoung@neo.tamu.edu

D. Song
e-mail: dzsong@cse.tamu.edu

**Keywords** Radio frequency localization · Wireless sensor network · Robot navigation · Particle filter

## 1 Introduction

Consider a scenario that our enemy has deployed a sensor network to detect troop movements in a desert. In order to neutralize the treat, we need to localize sensor network nodes. Since the sensor network is usually composed of a large number of miniature wireless sensor nodes with self-configurable ad hoc networking capabilities, localization of those nodes manually is difficult and time-consuming. Imagine that a mobile robot equipped with a highly sensitive directional radio antenna has been dispatched for the localization task. A new research problem arises because the networked configuration and packet information of the sensor network are unknown to the robot.

Due to the hardware and energy constraints, most of sensor network nodes employ carrier sensing multiple access (CSMA)-based Media Access Control (MAC) protocol or its variations. This allows us to take advantage knowledge of the CSMA MAC protocol in the localization process. However, localizing an unknown wireless sensor network is different and more difficult than localizing a constant radio beacon due to the unknown network size, transient and intermittent transmissions, and signal source anonymity.

As illustrated in Fig. 1, the robot can detect spatial distribution of radio signal strengths (RSS) as it travels in the field of radio sources. Our approach builds on augmented particle filters and combines a probabilistic sensing model that describes the characteristics of a directional antenna, and a CSMA model that can detect network configuration useful for localization purposes. The particle filters output the posterior probability distribution of radio sources. Based on the

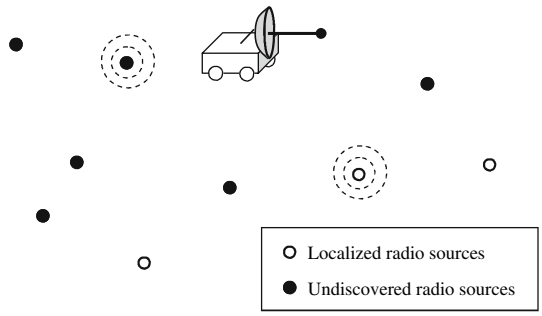


**Fig. 1** Schematics of deploying a single mobile robot to localize unknown wireless sensor network nodes. The nodes with *dashed circles* indicate that they are transmitting

particle distribution, we develop a motion planning scheme to generate robot control commands to search and localize radio sources. The final localization scheme consists of two algorithms: a sensing algorithm that runs in $O(n)$ time for $n$ particles and a motion planning algorithm that runs in $O(nl)$ time for $l$ radio sources. We have implemented the algorithm and the results show that the algorithms are capable of localizing unknown networked radio sources effectively and robustly.

The rest of the paper is organized as follows. We begin with related work in Sect. 2. We present system architecture and hardware in Sect. 3. Then we define the problem in Sect. 4. In Sect. 5, we introduce our sensing model. The robot motion planning problem is presented in Sect. 6. We validate our model and algorithm through simulation experiments in Sect. 7. Finally, we conclude the paper with Sect. 8.

## 2 Related work

Localization of unknown networked radio sources is related to a variety of research fields including radio frequency-based localization, Simultaneous Localization and Mapping (SLAM), modeling of radio antennas, and modeling of CSMA-based wireless network protocols.

The recent development of radio frequency-based localization can be viewed as the localization of "friendly" radio sources because researchers either assume an individual radio source that continuously transmits radio signals (similar to a lighthouse) [1–5] or assume that the robot/receiver is a part of the network which knows the detailed packet information [6–12]. However, such information is not always available in an unknown network. In a recent work [2], Letchner et al. use a network of wireless access points to localize a mobile unit. This can be viewed as a dual version of our problem. They use multiple static listeners to localize a mobile transmitter, while we try to localize multiple static transmitters using a mobile listener. In another closely related work [9], Sichitiu and Ramadurai localize sensor network nodes with a mobile beacon. Again, the mobile beacon and the sensor network nodes share the network information.

In robotics research, SLAM is defined as the process of mapping the environment and localizing robot position at the same time [13–17]. Although both SLAM and our research are based on Bayesian methods, SLAM assumes that the environment is static or close to static. Directly applying SLAM methods to our problem is not appropriate because networked radio sources create a highly dynamic environment where the signal transmission patterns change quickly. Although recent advances in SLAM allow tracking of moving objects [18] while performing SLAM tasks, the environment largely remains static. We realize that changes of transmission pattern are traceable because a large number of RF networks are based on a CSMA MAC layer protocol. Our work is inspired by particle filter-based SLAM methods which are capable of solving generic, non-Gaussian, and nonlinear problems.

Since a large class of wireless networks use a CSMA-based MAC layer protocol [19], we assume this as prior knowledge of the network. Utilizing a CSMA model to enhance sensing is a unique characteristic of our system. An early work by Malhotra and Krasniewski [3] uses multiple orthogonal antennas to triangulate the position of a radio source. Although they do not assume that the receiver understands more information other than the physical layer, their antenna model does not address cases when there is only one mobile antenna. Robot traveling constraint and perspective limitation are not the concern of their work.

This paper extends our previous conference paper [20] by providing detailed information on how to utilize particle filters and how robot motion planning is conducted based on the particle filter outcome, and presenting more experimental results. This work differs from our previous work [21] by considering signal retransmissions due to collisions.

## 3 System design

### 3.1 System architecture

Figure 2 illustrates the system architecture. Whenever the directional antenna intercepts a transmission, the RSS reading of the transmission enters the system along with the current robot/antenna configuration, which refers to the position and the orientation of the antenna. The robot knows its localization at any time in our system. The antenna model provides information to particle filters regarding the potential location of the radio source. The CSMA model updates its estimated number of potential radio sources, each of which corresponds to a particle filter. There are multiple parallel particle filters running with each of them corresponding to the spatial distribution of a potential radio source. Hence the

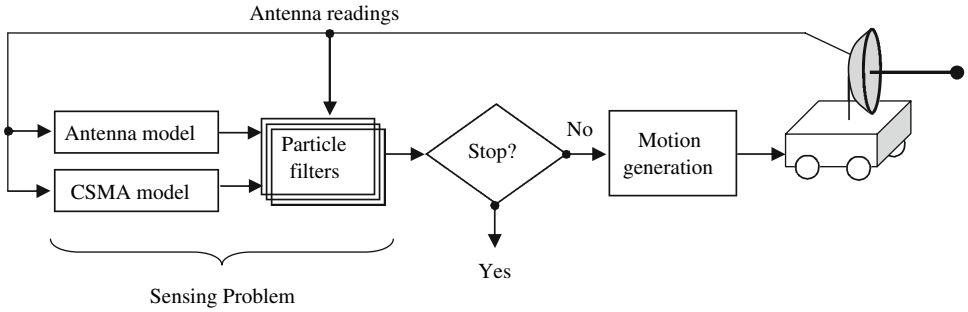


**Fig. 2** System architecture

spatial distribution of each radio source is represented by the particle distribution of each particle filter. The particle filters are updated based on the antenna model outputs. After each update of the particle filters the system determines if all radio sources are detected. If not, the motion generation algorithm plans robot motion to search for more radio sources.

### 3.2 Hardware

As illustrated in Fig. 3, the robot used in the system is custom made in our lab. The robot measures $50 \times 47 \times 50$ cm$^3$. The robot has two frontal drive wheels and one rear cast wheel and uses a typical differential driving structure. The robot can travel at a maximum speed of 50 cm/s. The radio sources are 2.4 GHz XBee nodes from Maxstream. Each XBee node has a chip antenna and the transmission power of 1 mW.

The directional antenna is a HyperGain HG2415G parabolic directional antenna with a maximum gain of 15 dBm at 2.4 GHz. It is an off-the-shelf product from L-com Global Connectivity Inc. Using directional antenna is an important design in acquiring bearing/directional information of unknown signal sources. The system utilizes both the RSS readings of the antenna and the orientation of the antenna as inputs. Since the antenna is fixed on the robot as illustrated in Fig. 3a, the antenna orientation is the same as the robot orientation.

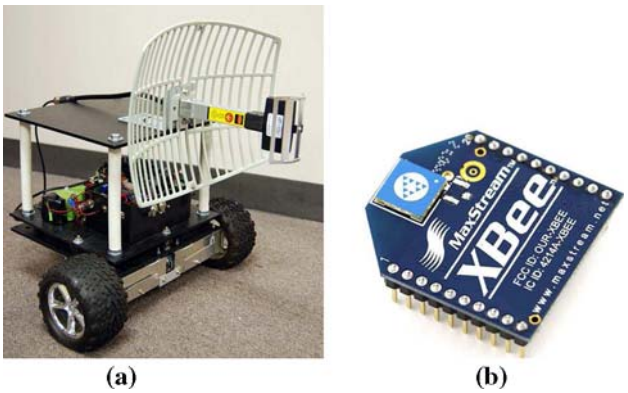


**Fig. 3** Hardware of the system. **a** The robot and the directional antenna. **b** Radio sources

It is important to point out that the unknown signal source may change the transmission power levels. For such cases, using an omni-directional antenna cannot provide correct correspondence between distance to the active radio source and RSS. Multiple antennas with different polarizations that form an antenna array should be used to find the direction of the unknown radio sources. In this case, RSS ratios between the antennas are more important than RSSs themselves. In recent work [22], Kim and Chong have shown how to find the radio source using two antennas with different polarizations. Since the focus of this paper is not on an antenna design or antenna array model, we use only one antenna to provide directional information by assuming fixed RSSs at transmitters for brevity. However, our method is not limited to this simple case and can be easily extended to a robot with an antenna array.

## 4 Problem definition

We are now ready to formulate our localization problem. To formulate the problem and focus on the most relevant issues, we have the following assumptions:

### 4.1 Assumptions

(1) The robot and radio sources are in a free and open 2D space. At this stage, we target at outdoor applications.
(2) The received radio signal does not contain information about the signal source. In fact, the robot usually cannot decode the packet at the MAC level due to the unknown network.
(3) Although the robot cannot decode the packets, it still can sense the collision of radio transmissions by monitoring RSS and phase changes.
(4) Network traffic is light and each transmission is short. These are the typical characteristics of a low power sensor network. Actually, this assumption makes localization more difficult. If the network traffic is heavy and the transmission duration is lengthy, the robot can localize the active radio source by simply "riding the wave."

In fact, most low power sensor nodes have a packet length magnitude of 10 ms.

(5) The directional antenna on the robot has high sensitivity and can listen to all traffic.

(6) The radiation pattern of the radio sources is circular. This assumption simplifies the modeling process. Later we will show that the proposed method also works for non-circular radiation patterns.

(7) The radio sources are stationary. At this stage, we do not consider mobile nodes.

(8) All radio sources transmit at the same power level. This assumption is not necessarily true for the most general case. For cases with different unknown power levels, we can use a pair of orthogonal antennas to extract directional information of the radio source regardless of the variation of transmission power level. Hence the proposed method can be easily generalized to cases with different transmission power levels.

(9) The robot can accurately execute its motion command. Our focus here is not to study the effect of imprecise motion.

Assumptions (2) and (3) differentiate localizing an unknown wireless sensor network node from localizing a "friendly" continuous radio beacon. Due to the transient and intermittent transmission pattern along with signal source anonymity, the robot cannot simply triangulate the signal source. Since only one robot is considered, the single perspective makes it more difficult than cases with multiple robots or receivers.

### 4.2 Nomenclature

- $k$: a discrete time index variable.
- $i$: a particle index variable, $i \in \mathbf{I} = \{1, \ldots, n\}$, where $n$ is the total number of particles and $\mathbf{I}$ is the particle index set. $n \leq n_{\max}$ is not a fixed number, where $n_{\max}$ is maximum number of particles.
- $m$: an index variable for radio sources, $m \in \mathbf{M} = \{1, \ldots, l\}$, where $l$ is the total number of radio sources and $\mathbf{M}$ is the radio source index set.
- $\mathbf{x}_m^k$: the estimated location of the $m$th radio source at time $k$. The variable is a random state variable because we do not know the actual location.
- $\mathbf{X}^k$: the joint state for all radio sources at time $k$, $\mathbf{X}^k = \{\mathbf{x}_1^k, \ldots, \mathbf{x}_l^k\}$.
- $\mathbf{s}_m^k$: a set of particles for the $m$th radio source, $\mathbf{s}_m^k = \{w_{m,i}^k, \vec{x}_{m,i}^k | i \in \mathbf{I}\}$, where each particle has an assigned relative weight $w_{m,i}^k$ and a potential radio source location $\vec{x}_{m,i}^k = [x_{m,i}^k, y_{m,i}^k]^T \in \mathbb{R}^2$.
- $\mathbf{S}^k$: the joint particle set at time $k$, $\mathbf{S}^k = \{\mathbf{s}_1^k, \ldots, \mathbf{s}_l^k\}$.
- $Z^k$: the RSS reading at time $k$, $Z^k \in [1, 255] \cap \mathbb{N}$.
- $\mathbf{Z}^k = \{Z^1, Z^2, \ldots, Z^k\}$: the set of all RSS values at time $k$.
- $\mathbf{u}^k$: a robot/antenna position and orientation at time $k$, $\mathbf{u}^k = [x^k, y^k, \theta^k]^T \in \mathbb{R}^2 \times \mathbb{S}$, where $\mathbb{S} = (-\pi, \pi]$ is the orientation angle set.

### 4.3 Problem definition

Based on the assumptions, we define our localization problem as follows.

*Problem 1* (Localization problem) Given all received RF signal strengths $\mathbf{Z}^k$, compute the number of radio sources, $l$, and estimate the position of each radio source $\mathbf{X}^k$.

Since we apply a particle filter approach to address the problem, properly designed particle filters should represent the spacial distribution of $\mathbf{X}^k$. Hence the overall problem can be broken down into the following two subproblems.

*Problem 2* (Sensing problem) Given all received RF signal strengths $\mathbf{Z}^k$, compute the number of radio sources, $l$, and the conditional probability of sensor locations $p(\mathbf{X}^k|\mathbf{Z}^k)$.

*Problem 3* (Motion planning problem) Given $p(\mathbf{X}^k|\mathbf{Z}^k)$, plan $\mathbf{u}^{k+1}$ for the $k+1$-th period.

## 5 Sensing problem

The sensing problem is to compute $p(\mathbf{X}^k|\mathbf{Z}^k)$. As illustrated in Fig. 2, there are three major components in the sensing problem: antenna model, CSMA modeling, and particle filters.

### 5.1 Antenna model

From antenna theory, bearing and distance are the two most important variables that determine the radiation pattern distribution in the 2D space for a given antenna. Recall that $\mathbf{u}^k = [x^k, y^k, \theta^k]^T$ is the robot antenna configuration when the radio transmission is sensed at time $k$ and $\mathbf{x}_m^k = [x_m, y_m]^T$ is the $m$th radio source position. Define $d_m^k$ and $\phi_m^k$ as the distance and the bearing from robot to the $m$th radio source position, respectively,

$$d_m^k = \sqrt{(x^k - x_m)^2 + (y^k - y_m)^2},$$
$$\phi_m^k = \operatorname{atan2}(x^k - x_m, y^k - y_m) - \theta^k.$$

Also from antenna theory [23], when the $m$-th radio source is transmitting, the expected RSS $Z^k$ of the directional antenna is approximated as,

$$E(Z^k) = 10 \left\{ \log_{10} C - \beta \log_{10}(d_m^k) + \log_{10} s(\phi_m^k) \right\}, \quad (1)$$

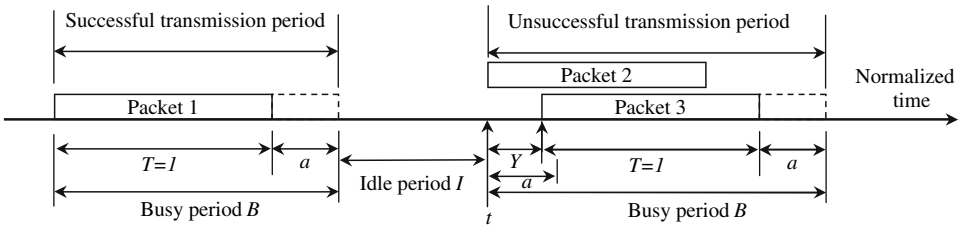


**Fig. 4** CSMA: transmission period analysis

where $C$ is a constant depending on radio transmission power and $(d_m^k)^{-\beta}$ is the signal decay function. The directivity of the antenna is captured by the term $s(\phi_m^k)$, which describes the radiation pattern of the antenna. We obtain $C = 1.77$ and the decay factor $\beta = 2.65$ from antenna calibration. Our $\beta$ value conforms to the widely-accepted notion that the decay factor is between 2 and 4 [23]. The units of $E(Z^k)$ are dBm. From antenna theory and the results from antenna calibration, we perform curve-fitting to obtain the radiation pattern function,

$$s(\phi_m^k) = \begin{cases} \cos^2(4\phi_m^k), & \text{if } -20^\circ \le \phi_m^k \le 20^\circ \\ \cos^2(80^\circ), & \text{otherwise.} \end{cases} \tag{2}$$

Equations (1) and (2) describe the expected RSS given that the radio transmission is from $m$-th radio source. However, the sensed RSS is not a constant but a random variable due to the uncertainties in radio transmissions. From the antenna calibration, we know that $Z^k$ conforms to the truncated normal distribution with a density function of

$$g(z) = \frac{\frac{1}{\sigma} f(\frac{z - E(Z^k)}{\sigma})}{F(\frac{z_{\max} - E(Z^k)}{\sigma}) - F(\frac{z_{\min} - E(Z^k)}{\sigma})}, \tag{3}$$

where the value of $\sigma$ is 3.3 by the antenna calibration, $z$ is the sensed RSS, $f(\cdot)$ is the probability density function (PDF) of a normal distribution with zero mean and unit variance, $F(\cdot)$ is the cumulative distribution function (CDF) of $f(\cdot)$, and $z_{\min}$ and $z_{\max}$ are the minimum and the maximum RSS that the antenna can sense, respectively. Let

$$G(z) = \int_{z_{\min}}^{z} g(z)\mathrm{d}z \tag{4}$$

be the CDF of the truncated normal distribution.

Since $Z^k$ can only take integer values, we obtain the antenna model as follows,

$$P(Z^k = z|\mathbf{x}_m^k) = G(z + 0.5) - G(z - 0.5). \tag{5}$$

### 5.2 CSMA model

One critical part of the sensing problem is to estimate how many radio sources are in the network. Here we utilize the CSMA model to estimate the potential number of sources.

Figure 4 illustrates the timing of a CSMA protocol. The time axis is alternatively divided into busy and idle periods. In the figure, $a \ll 1$ denotes the propagation delay, $t$ is the starting time of a busy period, and $t + Y$ is the time that the last packet arrives between $t$ and $t + a$, $0 < Y \le a$. $B$, $I$, and $U$ are the durations of the busy period, the idle period, and the time during a cycle that the channel is used without conflicts, respectively. Each busy period is also termed as a transmission period, which is further classified as a successful transmission period or an unsuccessful transmission period.

Without loss of generality, we set packet length $T = 1$ in Fig. 4. A packet takes additional time $a$ to propagate. Therefore, a successful transmission takes time $(1+a)$. $a$ is mainly determined by how fast the circuitry can recognize the transmission. If a radio source transmits packet 2 at time $t$, then the duration between $t$ and $t+a$ is a "vulnerable" period because other radio sources cannot sense its transmission and may initiate another transmission (Packet 3), which would lead to a collision.

If each radio source transmits according to an independent Poisson process with the same packet generation rate $\lambda$, the aggregated transmission rate $S$ is given by $S = l\lambda$. Due to retransmission, the actual packet arrival rate $G$, called offered traffic rate, is larger than $S$. By the aggregation of several Poisson signal sources, $S$ is also a Poisson process. $G$ can also be approximated with a Poisson process. The offered traffic rate $G$ is the sum of the source traffic rate $S$ and the retransmission traffic rate $R$, namely, $G = S + R$.

Define the busy collision probability $P_{pc}$ as the conditional probability of a collision given the channel is busy. Then

$$P_{pc} = 1 - e^{-aG} \tag{6}$$

by the approximation that $G$ is Poisson. Since the robot can listen to all traffic, $G$ and $P_{pc}$ can be observed over time. Hence the unknown networked parameter $a$ can be estimated using (6). We treat $a$ as known in the rest of the paper. Upon each collision, there are two retransmissions scheduled $R = 2GP_{pc}$. Therefore,

$$G = S + 2GP_{pc}. \tag{7}$$

With observed $G$ and $P_{pc}$, we can obtain $S$ using (7). If we know $\lambda$, then we can obtain $l = S/\lambda$. However, this would

not work for the most general cases because (1) $\lambda$ is usually unknown and (2) $\lambda$ might not be the same across different radio sources. To handle these issues, we can envision that each radio source can be further divided into multiple collocated sub radio sources with each sub radio source shares the same transmission rate $\lambda' << \lambda_{\min}$, where $\lambda_{\min}$ is the smallest transmission rate of the original radio sources.

Hence we can still apply the condition that each radio source has the same transmission rate of $\lambda'$. The number $l$ will be much bigger than the actual $l$. However, this is not a concern because we can always combine collocated sources after they are localized. For this reason, we assume each radio source shares the same transmission rate in the rest of the paper.

## 5.3 Particle filters

We now know that there are $l$ radio sources. For each radio source $m$, we use a particle filter to track its spacial distribution $p(\mathbf{x}_m^k|Z^k)$. This is an instance of the Bayes filtering problem which can be computed using a two-phase recursive approach:

1. Prediction phase:

$$p\left(\mathbf{x}_m^k|Z^{k-1}\right) = \int p\left(\mathbf{x}_m^k|\mathbf{x}_m^{k-1}, \mathbf{u}^k\right) p\left(\mathbf{x}_m^{k-1}|Z^{k-1}\right) \mathrm{d}\mathbf{x}_m^{k-1}. \tag{8}$$

Since positions of radio sources are static, state $\mathbf{x}_m^k$ is independent of the deterministic robot motion $\mathbf{u}^k$. Therefore, the prediction phase in (8) is trivial,

$$p\left(\mathbf{x}_m^k|Z^{k-1}\right) = p\left(\mathbf{x}_m^{k-1}|Z^{k-1}\right). \tag{9}$$

2. Update phase:

$$\begin{aligned} p\left(\mathbf{x}_m^k|Z^k\right) &= \eta p\left(Z^k|\mathbf{x}_m^k\right) p\left(\mathbf{x}_m^k|Z^{k-1}\right) \\ &= \eta p\left(Z^k|\mathbf{x}_m^k\right) p\left(\mathbf{x}_m^{k-1}|Z^{k-1}\right), \end{aligned} \tag{10}$$

where $\eta$ is a normalizing factor.

The particle filter represents $p(\mathbf{x}_m^k|Z^k)$ by a set of particles $\mathbf{s}_m^k$. Recall that $\mathbf{s}_m^k = \{w_{m,i}^k, \vec{x}_{m,i}^k | i = 1, \ldots, n\}$ where $n$ is the total number of particles, $w_{m,i}^k$ is the assigned weight for the particle, and $\vec{x}_{m,i}^k = [x_{m,i}^k, y_{m,i}^k]^T \in \mathbb{R}^2$ is the potential radio source location.

The update phase in the particle filters is performed in two stages: importance sampling and resampling.

### 5.3.1 Importance sampling

The importance sampling weights each of the samples

$$w_{m,i}^k = w_{m,i}^{k-1} p\left(Z^k|\vec{x}_{m,i}^k\right) \tag{11}$$

by the sensor model $p(Z^k|\vec{x}_{m,i}^k)$ that can be computed using (5). Each particle in $\mathbf{s}_m^k$ is randomly drawn from $\mathbf{s}_m^{k-1}$ proportional to the updated weight $w_{m,i}^k$. The importance sampling step reduces the number of low weighted particles and increases the number of high weighted particles.

### 5.3.2 Resampling

After a few iterations of the importance sampling, the number of survived particles shrinks and ultimately becomes zero, which causes the degeneracy problem. The problem can be solved by adding more particles into $\mathbf{s}_m^k$ by resampling when the effective number of particles is below an effective threshold number. Let $n_{\text{eff}}$ denote the effective number, which is computed based on weights,

$$n_{\text{eff}} = \frac{1}{\sum_{i=1}^n (w_{m,i}^k)^2} \tag{12}$$

according to [24]. We define $n_t$ as the threshold that is determined by the experiments. If $n_{\text{eff}} < n_t$, we perform resampling.

Resampling also introduces the problem of loss of diversity among particles. This is because samples are drawn from a discrete particle set rather than from a continuous distribution. To solve this problem, it is necessary to modify the resampling process by introducing Gaussian random noise into the resampled particles. Let $N(\vec{\mu}_r, \Sigma_r)$ denote the two dimensional Gaussian distribution, where $\vec{\mu}_r$ and $\Sigma_r$ are the mean vector and the covariance matrix, respectively. We take $\vec{\mu}_r = \vec{x}_{m,i}^{k-1}$ and $\Sigma_r$ is a tunable diagonal matrix determined by experiments. Therefore, particles in $\mathbf{s}_m^k$ are obtained by resampling from $\{w_{m,i}^k, N(\vec{x}_{m,i}^{k-1}, \Sigma_r) | i = 1, \ldots, n\}$.

Another potential issue of resampling is that there could be no particle in vicinity of the correct state. This is known as the *particle deprivation problem*. To address the problem, we add a 5% randomly generated particles into $\mathbf{s}_m^k$ with an initial weight of $1/n$ each.

## 5.4 Data association

For $l$ radio sources, there are $l$ particle filters. It is important to determine which particle filter to be updated once a RSS is perceived. This is a data association problem. We use maximum a posteriori probability (MAP) estimation to address the problem. Let $\hat{p}(\mathbf{x}_m^k|Z^k)$ be the posterior probability

estimation of the $m$th particle set,

$$\hat{p}(\mathbf{x}_m^k|Z^k) = \frac{\sum_{i=1}^{n} w_{m,i}^{k-1} p(Z^k|\vec{x}_{m,i}^{k-1})}{\sum_{j=1}^{l}\sum_{i=1}^{n} w_{j,i}^{k-1} p(Z^k|\vec{x}_{j,i}^{k-1})}. \quad (13)$$

Let $m^*$ be the index for the selected radio source, which is chosen by maximizing $\hat{p}(\mathbf{x}_m^k|Z^k)$,

$$m^* = \arg\max_{m\in\mathbf{M}} \hat{p}(\mathbf{x}_m^k|Z^k). \quad (14)$$

### 5.5 Stopping time and localization criterion

With the MAP approach, we can selectively update an individual particle filter. Figure 5 illustrates the results of the particle distribution with respect to the actual radio source location over time $k$. It is clear that the majority of particles converge to the vicinity of the radio source location. As a Monte Carlo method, it is necessary to determine a stopping time that detects convergency trend of the particles as a function of each individual particle set $\mathbf{s}_m^k$.

Since particles are located in the 2D space, the spatial distribution of particles in $\mathbf{s}_m^k$ can be described by a mean vector $\vec{\mu}_m$ and a covariance matrix $\Sigma_m$. Hence we have,

$$\vec{\mu}_m^k = \sum_{i=1}^{n} w_{m,i}^k \vec{x}_{m,i}^k, \quad (15)$$

$$\Sigma_m = \frac{\sum_{i=1}^{n} w_{m,i}^k \left[(\vec{x}_{m,i}^k - \vec{\mu}_m^k)(\vec{x}_{m,i}^k - \vec{\mu}_m^k)^T\right]}{1 - \sum_{i=1}^{n}(w_{m,i}^k)^2}. \quad (16)$$

Define $\lambda_m$ and $\mathbf{V}_m$ as the maximum eigenvalue and the corresponding eigenvector of $\Sigma_m$, respectively. According to principle component analysis (PCA), we know that the maximum variance of the particle distribution in the 2D space can be measured by its largest eigenvalue $\lambda_m$. As the particle set converges to the vicinity of the radio source, $\lambda_m$ should decrease. Define $\epsilon$ as the threshold for $\lambda_m$. We define that the $m$th radio source is located and we can stop the corresponding particle filter computation if

$$\lambda_m \leq \epsilon. \quad (17)$$

### 5.6 Algorithm

The computation of the sensing model can be summarized in Algorithm 1. It is clear that each iteration of Particle Filter-based Sensing Algorithm (PFSA) runs in $O(n)$ time for $n$ particles.

## 6 Motion planning problem

As illustrated in Fig. 5, the particle sets track the spatial distribution of radio sources. However, the results shown in Fig. 5 are based on a robot performing a random walk, which is not necessarily the best choice for robot motion planning. We need to develop an effective robot motion planner to ensure $\mathbf{s}_m^k$ converges.

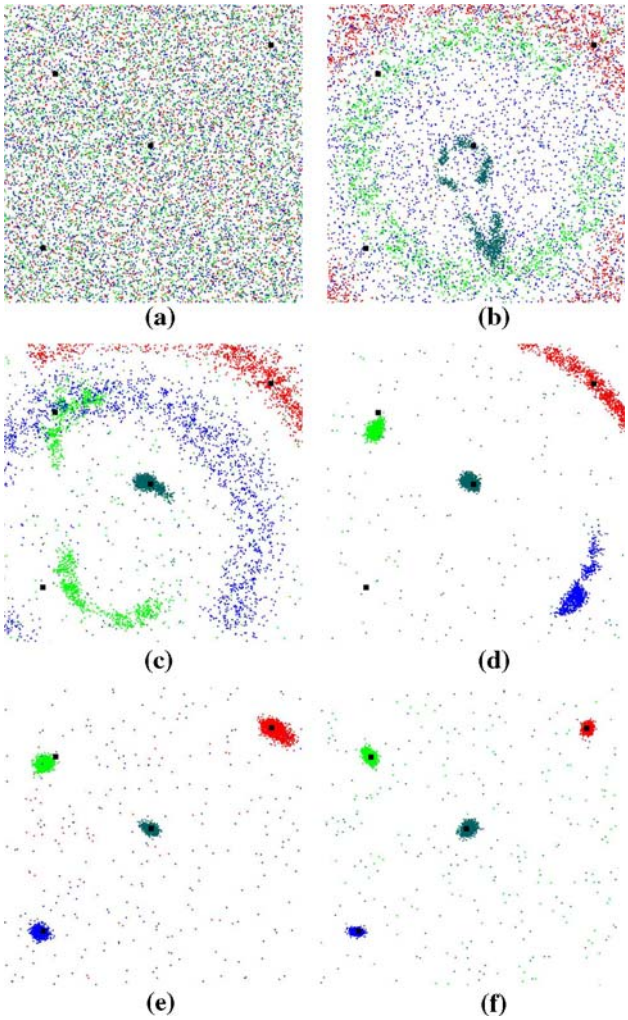


**Fig. 5** Sample results of particle distribution with respect to actual radio source location over time $k$. There are four radio sources represented by *black dots*. The smaller *color dots* indicate each individual particle. Four different *colors* represent results of four particle filters. The robot performs random walk in this example. **a** $k = 0$, **b** $k = 3$, **c** $k = 8$, **d** $k = 25$, **e** $k = 48$, **f** $k = 110$

We propose a two-step approach. First, the robot chooses a targeted radio source $m_t$ in terms of convergence and traveling distance. Then the robot determines its configuration that best ensures the convergence of $\mathbf{s}_{m_t}^k$.

### 6.1 Choosing a target source

The process of choosing a target largely depends on how well each particle set converges and the traveling distance of the robot. For the $m$-th particle set, recall that a smaller $\lambda_m$ means radio source $m$ is closer to be localized. Hence, the robot can

**Algorithm 1**: Particle Filter-based Sensing Algorithm

**input** : $\mathbf{Z}^k$
**output**: $\mathbf{s}_m^k$
**begin**

| | |
|---|---|
| Update $G$ | $O(1)$ |
| Estimate $S$ and $l$ according to (7) | $O(1)$ |
| Compute $\hat{p}(\mathbf{x}_m^k \mid Z^k)$ using (13) | $O(n)$ |
| Find $m^*$ using (14) | $O(1)$ |
| Compute $w_{m^*,i}^k$, $i \in \mathbf{I}$, using (11) | $O(n)$ |
| Normalize $w_{m^*,i}^k$, $i \in \mathbf{I}$ | $O(n)$ |
| $n_c = 0$; $\mathbf{s}_{m^*}^k = \emptyset$ | $O(1)$ |
| **for** $i = 1$ **to** $n$ **do** | $O(n)$ |
| Draw $i$ from $\mathbf{s}_{m^*}^{k-1}$ with probability $\propto w_{m^*,i}^k$ | $O(1)$ |
| **if** $\{w_{m^*,i}^k, \vec{x}_{m^*,i}^{k-1}\} \notin s_{m^*}^k$ **then** | |
| $\mathbf{s}_{m^*}^k = \mathbf{s}_{m^*}^k \cup \{w_{m_c,i}^k, \vec{x}_{m_c,i}^{k-1}\}$ | $O(1)$ |
| $n_c = n_c + 1$ | $O(1)$ |
| $n = n_c$ | $O(1)$ |
| Compute $n_{\text{eff}}$ using (12) | $O(1)$ |
| **if** $n_{eff} < n_t$ **then** | |
| **for** $i = 1$ **to** $95\% n_{\max}$ **do** | $O(n)$ |
| Draw particle $i$ from $\{w_{m^*,i}^k, N(\vec{x}_{m^*,i}^{k-1}, \Sigma_r) \mid i = 1, ..., n\}$ | $O(1)$ |
| Add the particle to $\mathbf{s}_{m^*}^k$ | $O(1)$ |
| $n_c = n_c + 1$ | $O(1)$ |
| Add $5\% n_{\max}$ random particles to $\mathbf{s}_{m^*}^k$ | $O(n)$ |
| $n = n_{\max}$ | $O(1)$ |
| Compute $\lambda_{m^*}$ using PCA | $O(1)$ |
| **if** $\lambda_{m^*} \leq \epsilon$ **then** | |
| radio source $m^*$ is localized. | $O(1)$ |

**end**

localize the target without spending too much time. On the other hand, we would like the robot to travel the minimum distance to save energy. We define the following function to describe the tradeoff between the convergence status and the traveling distance,

$$\omega_m = \alpha \lambda_m + (1 - \alpha) d_{\mu_m}, \tag{18}$$

where $0 \leq \alpha \leq 1$ is the weighting factor between convergence and distance, and $d_{\mu_m}$ is the distance between the robot's current position and the estimated position of $m$th radio source $\vec{\mu}_m^k$.

A radio source with a small $\omega_m$ would be a desirable target for the robot. However, if we use this metric, the robot might stick with a prominent target and fail to explore other targets. To avoid this, we define a history weighting function,

$$h(m_c) = \begin{cases} \infty & \text{if } \tau_{m_c} > \tau_{\max} \\ 1 & \text{otherwise} \end{cases} \tag{19}$$

where $m_c$ is the current target, $\tau_{m_c}$ is the elapsed time that the robot has been with the current target, and $\tau_{\max}$ is the time threshold for the maximum investigation duration. At each step, $\tau_{m_c}$ is updated as follows,

$$\tau_{m_c} = \begin{cases} \tau_{m_c} + 1 & \text{if } m_c \text{ has not change} \\ 0 & \text{otherwise.} \end{cases} \tag{20}$$

Therefore, the robot is forced to investigate other targets once $\tau_{\max}$ is reached. $\tau_{\max}$ can be obtained using the transmission rate $\lambda$ and a probability threshold $p_m$. The probability that the targeted radio source does not transmit any signal during $\tau_{\max}$ is $1 - e^{-\lambda \tau_{\max}}$. If we want the probability to be less than $p_m$, we can choose

$$\tau_{\max} = -\frac{1}{\lambda} \ln(1 - p_m). \tag{21}$$

Combining convergence, traveling distance, and history, we choose the targeted radio source $m_t$ that minimizes the following

$$m_t = \arg \min_{m \in \mathbf{M}} h(m_c) \omega_m. \tag{22}$$

### 6.2 Robot configuration

Once a target radio source $m$ is identified, we need to identify a corresponding robot configuration that can accelerate the convergence of the particle set $\mathbf{s}_m^k$. As illustrated in Fig. 6, an intuitive choice is to align the most sensitive reception region of the directional antenna with the particle set. In this way, the robot does not need to travel too close to the radio source, the robot can reduce its travel distance, and be energy efficient.

To ensure a good alignment between the antenna and the particle ellipsoid describing regions with a high concentration of particles, it is necessary to align the zero bearing angle of the antenna with the long axis of the particle ellipsoid. Recall that $\mathbf{V}_m$ represents the eigenvector that corresponds to the maximum eigenvalue of matrix $\Sigma_m$. Let $v_{m,x}$ and $v_{m,y}$ be the $x$- and $y$-components of $\mathbf{V}_m$, respectively. We know that the long axis of the ellipsoid is determined by $\mathbf{V}_m$ according to PCA. Hence, the orientation of the robot/antenna is,

$$\theta = \text{a tan } 2(v_{m,x}, v_{m,y}). \tag{23}$$

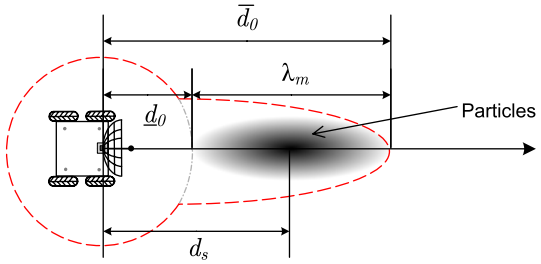


**Fig. 6** Sample robot configuration for a particle set. The *gray* ellipsoid region represents particle distribution. The *dashed red line* represents the directivity of the antenna (i.e., function $s(\cdot)$ in (2))

The remaining parameter is the distance between the robot and the center of the particles. As illustrated in Fig. 6, the distance is defined as $d_s$. If $d_s$ is obtained, the robot position $[x, y]$ is obtained,

$$x = \vec{\mu}_{m,x} - d_s \cos(\theta),$$
$$y = \vec{\mu}_{m,y} - d_s \sin(\theta), \tag{24}$$

where $\vec{\mu}_{m,x}$ and $\vec{\mu}_{m,y}$ represent the $x$- and $y$-components of $\vec{\mu}_m^k$, respectively. $\vec{\mu}_m^k$ is the center the particle set $\mathbf{s}_m^k$ according to (15). Therefore, we need to compute $d_s$. From PCA, we know that the ellipsoid in Fig. 6 is the approximation of the particle distribution. As illustrated in Fig. 6, we define $\overline{d}_0$ and $\underline{d}_0$ as the interception points of the outer and inner boundaries of the main reception area with the zero bearing axis, respectively. The boundary functions are described in (2). We would like to fit the long axis of the ellipsoid in between $\overline{d}_0$ and $\underline{d}_0$,

$$\lambda_m = \overline{d}_0 - \underline{d}_0. \tag{25}$$

Since $\lambda_m$ is known, this allows us to find the expected signal strength using (1),

$$E(Z) = 10\left[\log_{10} C - \beta \log_{10} \lambda_m + \beta \log_{10}\left(1 - 10^{\frac{\log_{10}\cos^2 80^\circ}{\beta}}\right)\right]. \tag{26}$$

The expected signal strength can help us to compute $\overline{d}_0$ and $\underline{d}_0$ and obtain

$$d_s = \underline{d}_0 + \frac{1}{2}\lambda_m. \tag{27}$$

Therefore, the robot configuration $[x, y, \theta]^T$ is found. As more transmission are intercepted, the particles converge and $\lambda_m$ decreases. Consequently, the robot adaptively moves close to the radio source to increase localization accuracy. Hence we name this approach as Greedy Adaptive Motion Planning (GAMP).

### 6.3 Algorithm

We summarize our GAMP algorithm in Algorithm 2. It is clear that the algorithm runs in $O(nl)$ time for $n$ particles and $l$ radio sources.

**Algorithm 2**: GAMP Algorithm

```
input : s_m^k
output : [x, y, θ]^T
begin
    for m = 1 to l do                                   O(l)
        Compute μ_m and Σ_m using (15) and (16)         O(n)
        Perform PCA on Σ_m and obtain λ_m               O(1)
    end
    Update τ_{m_c} using (20)                           O(1)
    Compute τ_max using (21)                            O(1)
    Compute ω_m using (18)                              O(1)
    Find m_t according to (22)                          O(1)
    Compute θ using (23)                                O(1)
    Compute E(Z) using (26)                             O(1)
    Compute d̄_0 and d̲_0 using (1)                       O(1)
    Compute d_s using (27)                              O(1)
    Compute [x, y, θ] using (24)                        O(1)
end
```

## 7 Experiments

We have implemented the algorithms and the simulation platform using Microsoft Visual C++. NET 2005 with OpenGL on a PC Desktop with an Intel 2.13 GHz Core 2 Duo CPU and 2 GB RAM. The machine runs Microsoft Windows XP. We are not able to run the actual physical experiment due to the range limitation of our local position system for the robot. GPS is not an option due to insufficient accuracy. To validate the results in high fidelity, we design a "hardware-in-the-loop" simulation where RSS readings are obtained from actual data by fixing the robot while moving the radio source around. Therefore, the simulation is driven by actual radiation patterns (except the case where we alter the radiation pattern for testing in non-circular transmission patterns). We call the data gathering processing as antenna calibration. In calibration, we have placed the radio source at 328 different orientations and distances with respect to the antenna. In each setting, we have collected 20 readings to measure the randomness of the reception. Those data are used to drive the simulation process.

For the unknown network, each radio source generates radio transmission signals according to an independently and identically distributed Poisson process with a rate of 0.01 packets per second. The packet length is 0.01 s. The propagation delay $a$ is 3% of the packet length. The radio sources are located in a square field with a side length of 30 m.

For the particle filter, we set the maximum number of particles for each radio source $n_{\max} = 3000$, the threshold for the effective number of particles $n_t = 1000$, and the covariance matrix for adding the Gaussian noise $\Sigma_r = \begin{pmatrix} \frac{1}{5} & 0 \\ 0 & \frac{1}{5} \end{pmatrix}$. For localization stopping condition, we set $\epsilon = 0.05$. For the motion planning, we set robot speed at 0.25 m/s, weighting factor $\alpha = 0.9$, and the probability threshold for transmission $p_m = 0.02$. Those parameters are set based on the best performance derived from multiple experiment trials.

### 7.1 A sample case

Figure 7 illustrates the robot trajectory and the convergence trends for a sample case with six radio sources. The initial

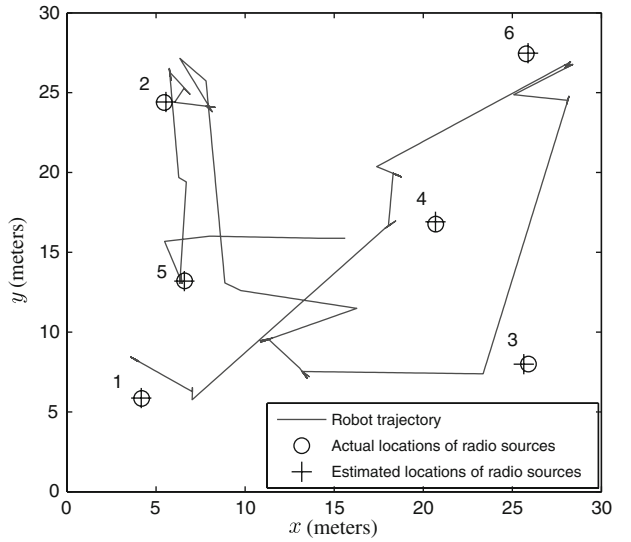


**(a)**

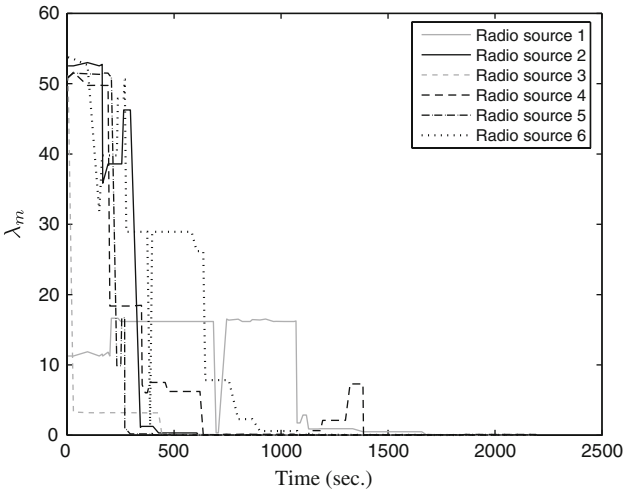


**(b)**

**Fig. 7** The resulting robot trajectory and the convergence trends for a sample case with six radio sources. **a** Trajectory, **b** convergence

position of the robot is the center of the field. As we can see from Fig. 7a, the robot gradually approaches each radio source. At the end of experiments, the estimated locations of radio sources are conformal to the actual locations of the radio sources. The localization process is successful. Figure 7b illustrates how $\lambda_m$ for each radio source converges over time. All $\lambda_m$'s successfully converge. What is worth noting is the relationship between the robot position and the convergence trend. If we take a close look at radio source 1, we can find that it converges last because it is the last radio source the robot approaches. We consider the convergence speed satisfactory because each radio source only transmits at a mean rate of 1 packet per 100 s.

For the sample case, the PFSA runs in 113 ms and GAMP algorithm runs in 0.6 ms. This is not surprising because they are linear algorithms. Since computation speed is not a concern here, we skip speed tests in the rest of experiments.

### 7.2 Comparison with two heuristic approaches

We also compare our GAMP to two heuristic approaches, namely, a random walk and a fixed-route patrol. The fixed-route patrol traverses the field using a pre-defined route. Since the robot has no knowledge of the localization of radio sources, the fixed route is usually the tour that traverse the entire region for coverage purpose. We increase the total radio source number $l$ from 2 to 8 to observe the performance of each method. For each trial, we randomly generate radio source locations and test all three methods. We repeat 20 trials for each case and compute the average time required for localizing all radio sources and the mean square error between estimated radio source locations and the actual source locations. Comparison results are shown in Fig. 8. All algorithms are able to localize radio sources. As illustrated Fig. 8a, GAMP is consistently faster than the two counterparts. As for the localization accuracy, Fig. 8b shows that all methods are similar in localization accuracy. The accuracy decreases as number of radio sources increases. We conjecture that this is due to the RSS resolution of the antenna and the randomness in RSS make all methods unable to distinguish the radio sources that are close to each other. Hence, the data association step in Sect. 5.4 might associate the radio source with a wrong particle filter and the accuracy of localization decreases.

### 7.3 Robustness tests

Our localization method is derived under a set of restrictive assumptions. In this part, we are interested in testing the system performance when relaxing some assumptions. In other words, we would like to know the robustness of the proposed method. Particularly, we focus on the most restrictive assumptions, which are Poisson arrival processes, circle radiation patterns, and evenly distributed traffic among radio sources.

The first test of robustness is to relax the assumption that the packets are generated according to Poisson processes. In reality, if a particular routing mechanism is used, then the packet generation processes could deviate significantly from Poisson processes. We simulate those traffic patterns by using Gaussian inter-arrival time. The Gaussian distribution has a mean of 0.01 s and a variance of 100. Other parameters are the same as the sample case test in Fig. 7. Figure 9a shows that our method is still consistently faster than its two counterparts. For localization accuracy, our method is slightly better. This indicates that our method is not limited to the Poisson arrival process.

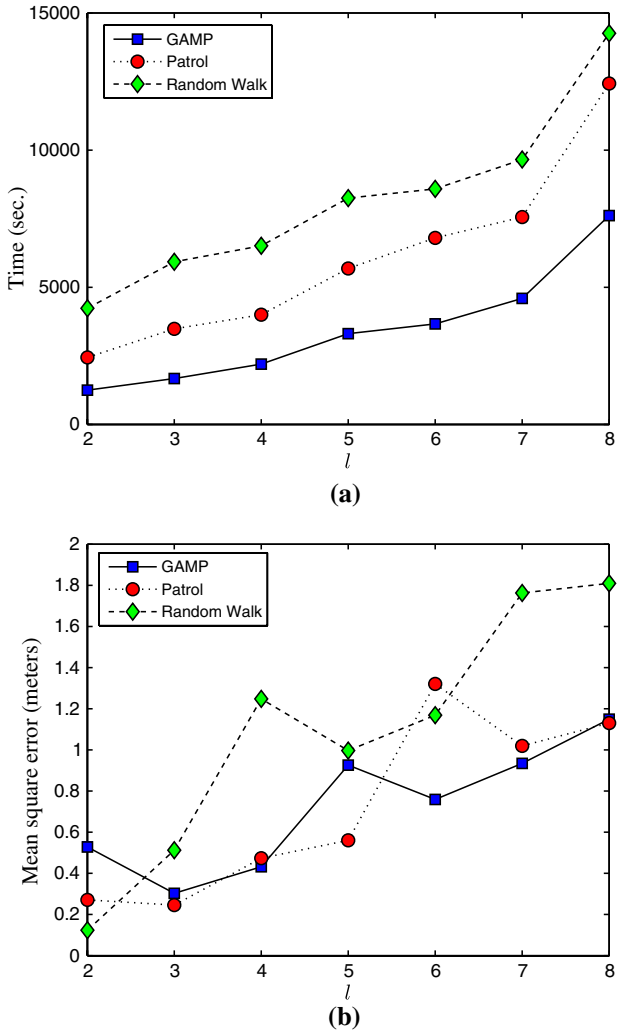


**Fig. 8** Localization performance comparison among the GAMP, a random walk, and a fixed route patrol. **a** Time comparison, **b** localization accuracy comparison

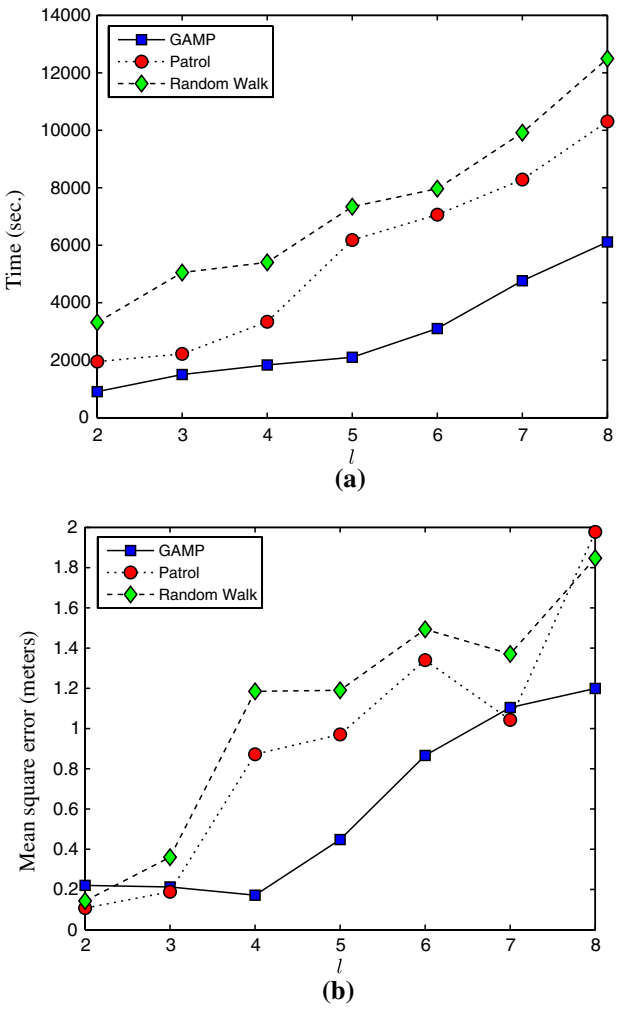


**Fig. 9** Localization performance comparison under Gaussian inter-arrival time. **a** Time comparison, **b** localization accuracy comparison

The second test of robustness concerns localization performance when the radiation pattern of the radio sources are non-circular. Due to different surface conditions, materials, and environment influence, the radiation pattern of a wireless sensor node is not necessarily circular. To characterize this problem, we use an ellipse radiation pattern to approximate the real radiation pattern. To quantify the deviation from the circular radiation pattern, we define axis ratio $r_a$ as the ratio between the minor axis and the major axis of the ellipse. If $r_a = 1$, the radiation pattern is perfectly circular. We vary the ratio from 0.2 to 1. We use a 6-radio source setup in the experiment and 20 random trials for each axis ratio. To avoid the possibility of failure to converge, we set the maximum running time of the simulation as 30,000 s. Figure 10 illustrates the results. Figure 10a shows that all three methods are very slow when $r_a$ is small and become fast when the axis ratio increases. When $r_a$ is small, the ellipse is long and narrow. Hence the antenna model cannot provide a reasonably accurate prediction of the location of the radio sources. Our GAMP method become faster than the other two when $r_a > 0.4$. Similar results in localization accuracy are shown in Fig. 10b. These results suggest that our GAMP method is more robust to non-circular radiation pattern than the other two, which is desirable. It is worth noting an ellipse model may not be able to characterize the strong irregularity of radiation patterns in some cases. For example, a bended antenna can cause its radiation pattern to be multi-modal instead of unimodal. In these cases, the algorithm has an decreased localization accuracy or may find some phantom sources. However, the results are still usable because they still significantly reduce the search space of the unknown radio sources.

The third test of the robustness focuses on the scenario where the traffic might be unevenly distributed in a sensor network. Due to the popularity of clustering techniques in

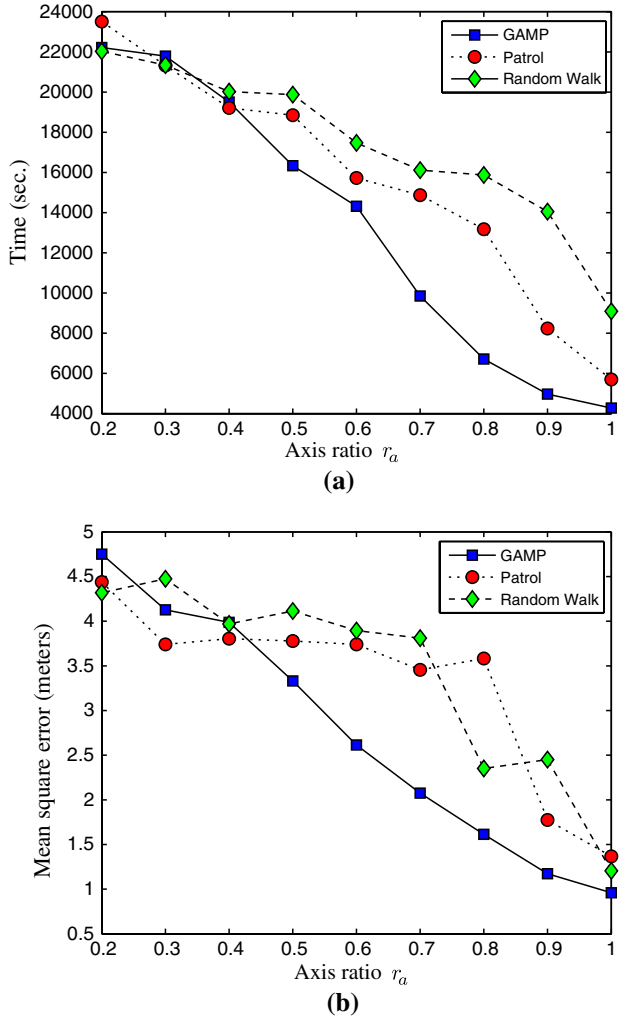


**Fig. 10** Localization performance comparison for a case with six radio sources and non circular radiation pattern. **a** Time comparison, **b** localization accuracy comparison

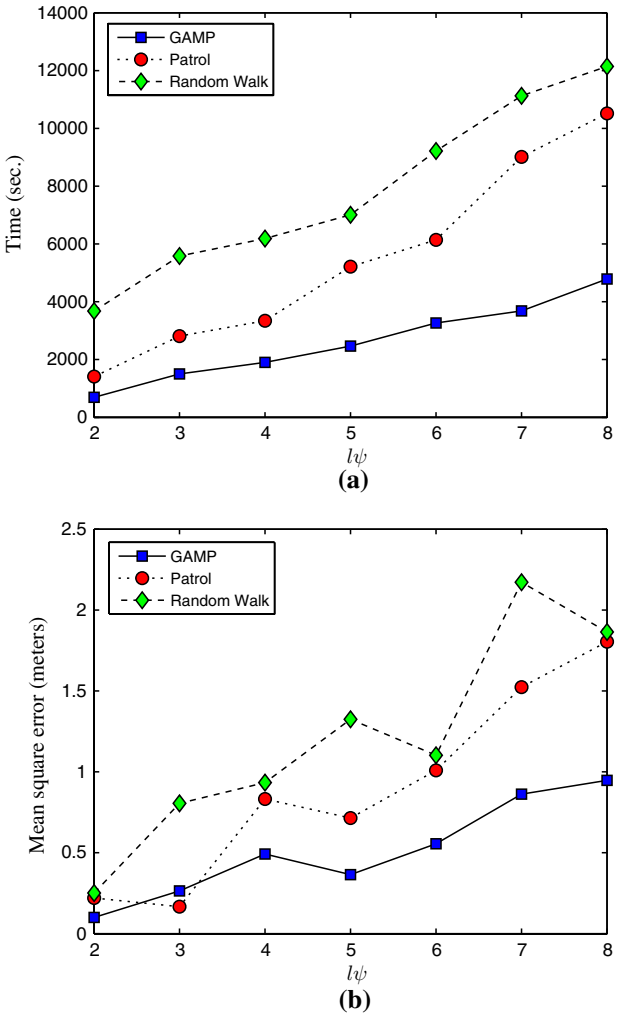


**Fig. 11** Localization performance comparison with uneven transmission rate. **a** Time comparison, **b** localization accuracy comparison

routing, certain nodes (i.e., cluster heads/routers) have much higher traffic than other nodes in the network. In this test, we set one radio source to transmit at 0.05 packets per second and other radio sources transmit at 0.01 packets per second. The rest of setup is the same as those in Fig. 8. Figure 11 illustrates the time and accuracy comparison results. Once again, our GAMP method is better than the other counterparts when the transmission rate is uneven.

All of the tests show that our localization method is more robust to the violation of assumptions than the fixed route patrol and the random walk.

## 8 Conclusions and future work

We reported how to use a single mobile robot equipped with a directional antenna to localize unknown networked radio sources. We proposed a particle filter-based localization approach that combines a CSMA model and a directional antenna model. We also proposed a motion planning algorithm based on the particle distribution. The sensing algorithm runs in $O(n)$ time for $n$ particles and the motion planning algorithm runs in $O(nl)$ time for $l$ radio sources and $n$ particles. We have implemented the algorithm and tested it using a real data-driven simulation platform. The results show that the algorithm is capable of localizing unknown networked radio sources. The experiment results shown that the proposed localization method is faster, more accurate, and more robust than the two other heuristic methods.

We are currently testing our algorithm using physical experiments. We are also interested in designing a multiple-robot localization scheme and will consider an approach to localize moving radio sources. Another important extension is to deal with scenarios where the radio source may change its transmission power during the communication.

## References


1. Bahl P, Padmanabhan VN (2000) RADAR: an in-building RF-based user location and tracking system. In: INFOCOM'00, pp 775–784
2. Letchner J, Fox D, LaMarce A (2005) Large-scale localization from wireless signal strength. In: Proceedings of the national conference on artificial intelligence (AAAI-05)
3. Malhotra N, Krasniewski M, Yang C, Bagchi S, Chappell W (2005) Location estimation in ad hoc networks with directional antennas. In: ICDCS '05: Proceedings of the 25th IEEE international conference on distributed computing systems (ICDCS'05). IEEE Computer Society, Washington, DC, USA, pp 633–642
4. Youssef M, Agrawala A, Shankar U (2003) WLAN location determination via clustering and probability distributions. In: IEEE PerCom 2003, p 143
5. Mao G, Fidan B, Anderson B (2007) Wireless sensor network localization techniques. Comput Netw 51(7):2529–2553
6. Bulusu N, Heidemann J, Estrin D (2000) GPS-less low cost outdoor localization for very small devices. IEEE Pers Commun Mag 7(5):28–34
7. Ji X, Zha H (2004) Sensor positioning in wireless ad-hoc sensor networks using multidimensional scaling. In: INFOCOM'04
8. Lorincz K, Welsh M (2005) Motetrack: a robust, decentralized approach to RF-based location tracking. In: Proceedings of the international workshop on Location and Context-Awareness (LoCA 2005) at pervasive 2005
9. Sichitiu M, Ramadurai V (2004) Localization of wireless sensor networks with a mobile beacon. In: First IEEE international conference on mobile ad hoc and sensor systems, pp 174–183
10. Bulusu N, Bychkovskiy V, Estrin D, Heidemann J (2002) Scalable, ad hoc deployable RF-based localization. In: Grace Hopper celebration of women in computing conference 2002, Vancouver, British Columbia, Canada. University of California at Los Angeles, October 2002 [Online]. Available: http://www.cs.ucla.edu/~bulusu/papers/Bulusu02a.html
11. Koutsonikolas D, Das S, Hu Y (2007) Path planning of mobile landmarks for localization in wireless sensor networks. Comput Comun 30:2577–2592
12. Sit T, Liu Z, Jr MA, Seah W (2007) Multi-robot mobility enhanced hop-count based localization in ad hoc networks. Robot Auton Syst 55:244–252
13. Thrun S (2002) Robotic mapping: a survey. In: Lakemeyer G, Nebel B (eds) Exploring artificial intelligence in the new millenium. Morgan Kaufmann, San Francisco
14. Dissanayake MWMG, Newman P, Clark S, Durrant-Whyte HF, Csorba M (2001) A solution to the simultaneous localization and map building (SLAM) problem. IEEE Trans Robot Autom 17(3):229–241
15. Hähnel D, Burgard W, Fox D, Fishkin K, Philipose M (2004) Mapping and localization with RFID technology. In: Proceedings of the IEEE International Conference on Robotics and Automation (ICRA)
16. Murphy KP (1999) Bayesian map learning in dynamic environments. In: NIPS, pp 1015–1021
17. Fox D, Thrun S, Dellaert F, Burgard W (2000) Particle filters for mobile robot localization. In: Doucet A, de Freitas N, Gordon N (eds) Sequential Monte Carlo methods in practice. Springer, New York
18. Wang C, Thorpe C, Thrun S, Hebert M, Durrant-Whyte H (2007) Simultaneous localization, mapping and moving object tracking. Int J Robot Res 26(9):889–916
19. Walrand J, Varaiya P (2000) High-performance communication networks, 2nd edn. Morgan Kaufmann, San Francisco
20. Song D, Yi J, Goodwin Z (2007) Localization of unknown networked radio sources using a mobile robot with a directional antenna. In: The American Control Conference (ACC), New York City, USA, July, 2007, pp 5952–5957
21. Song D, Kim C, Yi J (2009) Monte carlo simultaneous localization of multiple unknown transient radio sources using a mobile robot with a directional antenna. In: IEEE International Conference on Robotics and Automation (ICRA), Kobe, Japan, May 2009
22. Kim M, Chong NY (2009) Direction sensing RFID reader for mobile robot navigation. IEEE Trans Autom Sci Eng 6(1):44–54
23. Elliott RS (2003) Antenna Theory and Design. The IEEE Press, USA
24. Doucet A, Johansen AM (2008) A tutorial on particle filtering and smoothing: Fifteen years later. Tech. Rep